J Antimicrob Chemother 2018; **73**: 2104–2111
doi:10.1093/jac/dky143 Advance Access publication 10 May 2018

Journal of Antimicrobial Chemotherapy

Simultaneous population pharmacokinetic modelling of plasma and intracellular PBMC miltefosine concentrations in New World cutaneous leishmaniasis and exploration of exposure–response relationships

Anke E. Kip[1], María del Mar Castro[2], Maria Adelaida Gomez[2], Alexandra Cossio[2], Jan H. M. Schellens[3,4], Jos H. Beijnen[1,3,4], Nancy Gore Saravia[2] and Thomas P. C. Dorlo[1]*

[1]Department of Pharmacy & Pharmacology, Antoni van Leeuwenhoek Hospital/The Netherlands Cancer Institute, Amsterdam, The Netherlands; [2]Centro Internacional de Entrenamiento e Investigaciones Medicas (CIDEIM), Cali, Colombia; [3]Division of Pharmacoepidemiology & Clinical Pharmacology, Utrecht Institute for Pharmaceutical Sciences (UIPS), Faculty of Science, Utrecht University, Utrecht, The Netherlands; [4]Department of Clinical Pharmacology, Antoni van Leeuwenhoek Hospital/The Netherlands Cancer Institute, Amsterdam, The Netherlands

*Corresponding author. Department of Pharmacy & Pharmacology, Antoni van Leeuwenhoek Hospital/The Netherlands Cancer Institute, Amsterdam, The Netherlands, Plesmanlaan 121, 1066 CX, Amsterdam, The Netherlands. E-mail: t.dorlo@nki.nl

Received 26 August 2017; returned 5 December 2017; revised 21 December 2017; accepted 23 March 2018

Objectives: *Leishmania* parasites reside within macrophages and the direct target of antileishmanial drugs is therefore intracellular. We aimed to characterize the intracellular PBMC miltefosine kinetics by developing a population pharmacokinetic (PK) model simultaneously describing plasma and intracellular PBMC pharmacokinetics. Furthermore, we explored exposure–response relationships and simulated alternative dosing regimens.

Patients and methods: A population PK model was developed with NONMEM, based on 339 plasma and 194 PBMC miltefosine concentrations from Colombian cutaneous leishmaniasis patients [29 children (2–12 years old) and 22 adults] receiving 1.8–2.5 mg/kg/day miltefosine for 28 days.

Results: A three-compartment model with miltefosine distribution into an intracellular PBMC effect compartment best fitted the data. Intracellular PBMC distribution was described with an intracellular-to-plasma concentration ratio of 2.17 [relative standard error (RSE) 4.9%] and intracellular distribution rate constant of 1.23 day^{-1} (RSE 14%). In exploring exposure–response relationships, both plasma and intracellular model-based exposure estimates significantly influenced probability of cure. A proposed PK target for the area under the plasma concentration–time curve (day 0–28) of >535 mg·day/L corresponded to >95% probability of cure. In linear dosing simulations, 18.3% of children compared with 2.8% of adults failed to reach 535 mg·day/L. In children, this decreased to 1.8% after allometric dosing simulation.

Conclusions: The developed population PK model described the rate and extent of miltefosine distribution from plasma into PBMCs. Miltefosine exposure was significantly related to probability of cure in this cutaneous leishmaniasis patient population. We propose an exploratory PK target, which should be validated in a larger cohort study.

Introduction

Leishmania are protozoan parasites that cause the tropical disease leishmaniasis, which can result in diverse clinical manifestations, such as systemic infection (visceral leishmaniasis) or the skin lesions of cutaneous leishmaniasis. The parasites primarily reside and replicate in macrophages during infection of humans or other mammalian hosts. Hence, the direct target of antileishmanial drugs is inside macrophages, highlighting the relevance of the intracellular pharmacokinetics of these drugs.[1]

Miltefosine is currently the only registered oral drug for treatment of leishmaniasis. Several hypotheses exist for the mechanisms of action of miltefosine, including disturbance of lipid-dependent cell signalling and induction of mitochondrial dysfunction and apoptosis, which require macrophage membrane sequestering or cell entry of miltefosine.[2]

A large portion (57%) of total miltefosine has been found to be sequestered in the Caco-2 cell membrane after *in vitro* incubation, whereas only 7% was transported across the membrane.[3] Sequestered miltefosine in the outer membrane leaflet was

transported towards the inner leaflet by both passive and active transport mechanisms in the clinically observed range of miltefosine plasma concentrations.[3,4] Interindividual variability in saturation of the active inward translocation of miltefosine could potentially result in between-subject variability (BSV) in intracellular exposure of parasites to this drug.

Miltefosine pharmacokinetics have, until our recent study, only been described in plasma, in both cutaneous and visceral leishmaniasis patients.[5–7] Children with visceral leishmaniasis were found to be underexposed to miltefosine in comparison with adults when treated with the conventional linear, 28 day, 2.5 mg/kg daily dosing regimen. Furthermore, a relationship between miltefosine exposure and probability of final treatment cure was established in visceral leishmaniasis.[7] An allometric dosing regimen based on fat-free mass (FFM) was proposed to increase miltefosine exposure in children to adult levels, in order to increase the probability of cure.[6]

We previously conducted a pharmacokinetic (PK) clinical trial to compare the pharmacokinetics of miltefosine in paediatric and adult cutaneous leishmaniasis patients in Colombia, the results of which have recently been published.[1] The non-compartmental PK analysis (NCA) in that report contains the first known description of intracellular miltefosine exposure in PBMCs. Intracellular PBMC miltefosine steady-state concentrations were found to be around 2-fold higher than plasma concentrations, which could be clinically relevant with regard to miltefosine's intracellular mode of action. Lower miltefosine exposure in paediatric compared with adult patients was confirmed, both in plasma and intracellularly, but no exposure–response relationship could be discerned.[1]

The objective of the present study was to develop a population PK model with the data of the aforementioned study,[1] describing the kinetics of intracellular distribution of miltefosine in PBMCs by simultaneous modelling of plasma and intracellular PBMC concentrations. Using a non-linear mixed effects modelling approach, miltefosine exposure can be more accurately described than with NCA, particularly with the sparse sampling scheme achievable in young children.[8] Additionally, we explored the exposure–response relationship between plasma and intracellular PBMC exposure and treatment outcome and we simulated an allometric dosing regimen in both children and adults using the developed population PK model.

Patients and methods

Study population, PK sampling and bioanalysis

Data for this model-based analysis originated from an open-label clinical trial investigating the pharmacokinetics of 28 day 1.8–2.5 mg/kg daily miltefosine monotherapy for the treatment of cutaneous leishmaniasis patients (registered as NCT01462500). The non-compartmental PK data, toxicity and treatment outcomes have been published previously.[1] Sixty patients (30 adults and 30 children) were treated in two outpatient clinical facilities in Centro Internacional de Entrenamiento e Investigaciones Médicas (CIDEIM) in Cali and Tumaco, Colombia.[1] Cure was defined as complete re-epithelialization and absence of inflammatory signs for all lesions at the end of a 6 month follow-up period.

Plasma and PBMC samples were obtained from heparin anticoagulated peripheral blood collected pre-dose, after 1, 14 and 28 days of treatment, and during the follow-up period on day 60, 90, 120 and 210 after start of treatment. For PBMC isolation, the blood sample was diluted in PBS and placed over a Ficoll gradient.[9] In short, the mononuclear leucocyte layer was isolated after a 15 min 400 **g** centrifugation step at room temperature and washed twice with PBS. After an 800 **g** centrifugation step, the supernatant was removed and pellets were stored at −80°C. Plasma and PBMC samples were transported to the bioanalytical laboratory and stored at −20°C until analysis. Analysis was performed with LC–MS/MS.[1,9,10] Intracellular PBMC concentrations were calculated as described previously using the PBMC cell count and average cell volume.[9,11]

PK samples were available for 59 patients. Seven patients were excluded from the population PK analysis owing to potential non-adherence based on their PK profiles (>40% miltefosine decrease concentration during treatment).[1] One additional patient was excluded owing to missing dosing data, bringing the number of patients included in the population PK model to 51. Of these, two patients were lost to follow-up. As treatment outcome could not be evaluated for these patients, data from 49 patients were included in the exposure–response exploratory analysis.

Ethics

Ethics approval was obtained from the institutional ethics review board of CIDEIM and the Colombian National Institute for Food and Drug Safety (INVIMA). Written informed consent was obtained from each patient. Written informed consent was provided by the legal guardians of paediatric patients, and children >7 years old provided written informed assent.

Population PK analysis

Data management was performed in R (version 3.1.2) and Excel (Office 2007). Non-linear mixed effects modelling was performed with NONMEM (version 7.3) using a first-order conditional estimation procedure with interaction between interindividual variability and residual error components. Pirana (version 2.8.1) was used as an interface between NONMEM, Perl-speaks-NONMEM (PsN, version 3.4.2), R and the R-package Xpose (version 4.5.3) to evaluate model performance.

Minimization of the objective function value (OFV, minus twice the log likelihood) was used as a basic evaluation method to guide selection of a structural, stochastic and covariate model (selection criteria $\Delta OFV \geq 3.84$, $P<0.05$). Goodness of fit and predictive performance of the models were evaluated by graphical methods and visual predictive check (VPC) based on 1000 simulated replicates, respectively. A bootstrap (1000 samples) was performed to assess precision and reliability of the final parameter estimates. Shrinkage of empirical Bayes estimates and residual error components were evaluated.

Structural model

Population PK models were first evaluated using miltefosine plasma data only to identify the best structural model. A previously developed open two-compartment model with first-order absorption and linear elimination from the central compartment was taken as reference model from which further structural models were developed.[5,6] Subsequently, PBMC data were added to the data set to link intracellular to plasma data using an effect compartment strategy.[12,13] All final parameters for the structural model with plasma and PBMC data were estimated in a simultaneous fit.

The primary PK parameters estimated were CL (elimination clearance or intercompartmental clearance) and *V*. Both CL and *V* were expressed relative to bioavailability because the absolute bioavailability of miltefosine is unknown. Owing to limited sampling per dosing interval, the absorption rate (k_a) was fixed at 9.6 day^{-1}, based on previously reported values.[7]

Stochastic model

BSV in PK parameters was estimated with an exponential model. Residual variability was modelled with separate proportional errors for plasma and intracellular PBMC data as more variability is expected in PBMC compared with plasma separation.

Covariate model

Covariate selection was done using forward inclusion and backward elimination with the final structural PK model, with selection criteria of ΔOFV$\geq$3.84 ($P<0.05$) and $\geq$6.64 ($P<0.01$), respectively. Body weight and FFM were evaluated as covariates on *V* and CL. The population estimates for CL and *V* were scaled to a standard weight of 70 kg or FFM of 53 kg to make results comparable to previously published studies.[6,7] An allometric power function was used with a power of 0.75 for CL and 1 for *V* (representing linear scaling), based on a previously published population PK model.[6]

FFM was initially calculated as described in Equation 1 where HT is height (m), WT is weight (kg), WHS_{max} and WHS_{50} are the maximal and half-maximal weight for height standard (kg/m^2), respectively. WHS_{max} is 42.92 or 37.99 kg/m^2 and WHS_{50} is 30.93 or 35.98 kg/m^2 for males and females, respectively.[14]

$$FFM = WHS_{max} \cdot HT^2 \cdot \left(\frac{WT}{WHS_{50} \cdot HT^2 + WT}\right) \quad (1)$$

Owing to the large proportion of paediatric patients in this study, an age maturation component in FFM calculation was introduced (Equations 2 and 3),[15] estimating FFM with a sigmoid hyperbolic function asymptoting towards the predicted adult FFM described in Equation 1, with age and gender as additional covariates.

$$FFM\ (males) = \left[0.88 + \left(\frac{1-0.88}{\left[1+\left(\frac{AGE}{13.4}\right)^{-12.7}\right]}\right)\right] + \left[\frac{9270 \cdot WT}{6680 + \left(216 \cdot \frac{WT}{HT^2}\right)}\right] \quad (2)$$

$$FFM\ (females) = \left[1.11 + \left(\frac{1-1.11}{\left[1+\left(\frac{AGE}{7.1}\right)^{-1.1}\right]}\right)\right] + \left[\frac{9270 \cdot WT}{8780 + \left(244 \cdot \frac{WT}{HT^2}\right)}\right] \quad (3)$$

Model-based exposure estimates and exploring exposure–response relationships

AUC model-based estimates were calculated for each individual included in the population PK model by integrating the area under the individual model-based predicted miltefosine concentrations over time until day 28 of treatment (AUC_{D0-D28}) and infinity ($AUC_{0-\infty}$), both in plasma (AUC_{PL}) and intracellularly in PBMCs (AUC_{IC}). Of the 51 patients included, *Leishmania* strains were isolated from 37 patients, of which 89% corresponded to *Leishmania (Viannia) panamensis*. IC_{50} values were not determined in this study population. The median *ex vivo* IC_{50} of 1.9 mg/L found in clinical strains isolated from 11 patients from the same endemic region as participants from the present study, infected with *L.V. panamensis*,[16] was used to calculate the time>IC_{50} (total time the individual model-based predicted miltefosine concentration was above IC_{50}, in days) and AUC>IC_{50} (integration of area under individual model-based predicted concentration above IC_{50}, in mg·day/L).

The exposure–response relationships based on model-based estimates were explored with a logistic regression analysis in R. The logistic regression analysis was performed on a binary outcome (0=failure, 1=cure) as described in Equation 4 for $AUC_{PL,\ D0-D28}$ (in mg·day/L) as an example exposure variable. λ_i is the log odds of cure for the ith individual, λ_b represents the baseline log odds of cure and θ_1 describes the drug effect.

$$\lambda_i = \lambda_b + \theta_1 \cdot (AUC_{PL,\ D0-D28,\ i}) \quad (4)$$

Subsequently, λ_i was converted to probability of cure for the ith individual (p_i, Equation 5).

$$p_i = \frac{e^{\lambda_i}}{1 + e^{\lambda_i}} \quad (5)$$

Additional independent covariates available (baseline lesion size, lesion duration before treatment, number of lesions, sex, ethnicity and age) were evaluated as additional predictor variable next to the exposure variable, as described in Equation 6 with θ_2 describing the effect of the covariate (COV) on the log odds of cure for the ith individual.

$$\lambda_i = \lambda_b + \theta_1 \cdot (AUC_{PL,\ D0-D28,\ i}) + \theta_2 \cdot (COV_i) \quad (6)$$

Previously determined individual susceptibility data of isolated strains[1] based on the reduction of intracellular parasite burden at a concentration of 16 μM miltefosine *ex vivo*, were also evaluated as covariate in addition to drug effect as described in Equation 6. For 13/49 patients included in the exposure–response exploratory analysis, susceptibility data were unavailable and thus the median value was imputed.

Simulations of allometric dosing regimen

An allometric dose of miltefosine has previously been proposed for children with visceral leishmaniasis: a more optimal dosing schedule based on FFM, not linearly scaled but with a power exponent of 0.75, following allometric principles.[6] Drug exposure after allometric dosing was compared with conventional linear 2.5 mg/kg/day dosing. PK curves were simulated (n=1000) for patients with similar anthropometric characteristics as the subjects in the original data set. The allometric dose was based on FFM as calculated with Equations 2 and 3.[15] As an example, using these study participants' anthropometric characteristics, the allometric dose of subjects between 4 and 7 years old would lie between 2.8 and 3.2 mg/kg/day, as opposed to the standard 2.5 mg/kg dose. The 2.5 mg/kg/day dosing regimen and allometric dosing regimen were both rounded to the nearest 10 mg capsule, based on available formulations (10 or 50 mg).

Results

Patient and sample inclusion in population PK model

Demographic characteristics of the 51 study participants included in the population PK analysis are described in Table 1. Intracellular PBMC miltefosine concentrations on day 90 and afterwards were excluded from PK analysis because miltefosine concentrations for >80% of these samples were below the lower limit of quantification (<LLOQ). The drug concentration in one plasma sample was <LLOQ and was therefore excluded. Two PBMC and two plasma samples were excluded owing to the high absolute conditionally weighted residuals (CWRES>4). Finally, concentration data from 339 plasma and 194 PBMC samples were included in the population PK model.

Miltefosine population pharmacokinetics in plasma and intracellularly in PBMCs

Intracellular PBMC distribution appeared to be delayed, because the median intracellular-to-plasma ratio increased from 1.2, after the first day, to 2.9 after 28 days of treatment. Variability in observed intracellular PBMC concentrations was larger [relative standard deviation (RSD) 91%] compared with plasma concentrations (RSD 33%). This may partially be explained by higher variability in PBMC bioanalysis but might also be indicative of larger variability in miltefosine uptake between patients.

A three-compartment model significantly improved the fit (ΔOFV −232) compared with the previously developed two-compartment model,[6,7] as the latter overestimated concentrations on day 28 and 120. The model that best described the intracellular PBMC data was found to be miltefosine distribution to an intracellular PBMC effect compartment without mass transfer

Table 1. Demographics of patient population included in population PK model

Parameter	Adults	Children	All
Total no. of patients	22	29	51
Female patients, *n* (%)	12 (54.5)	12 (41.4)	24 (47.1)
Ethnicity, *n* (%)			
Afro-Colombian	17 (77.3)	21 (72.4)	38 (74.5)
Mestizo	5 (22.7)	8 (27.6)	13 (25.5)
Daily dose of miltefosine (mg/kg/day)	2.1 (1.4–2.8)	2.3 (2.0–2.5)	2.2 (1.4–2.8)
Age (years)	34 (21–51)	8 (2–12)	19 (2–51)
Body weight (kg)	71.1 (50.4–102)	26.5 (12.6–45.9)	45.7 (12.6–102)
Height (cm)	165 (152–182)	126 (92–153)	143 (92–182)
FFM (kg)[a]	48.3 (33.7–70.9)	20.6 (10.5–30.1)	32.6 (10.5–70.9)
Patients with treatment failure, *n* (%)	0 (0)	5 (17.2)	5 (9.8)
Treatment centres, *n* (%)			
Cali	8 (36.4)	8 (27.6)	16 (31.4)
Tumaco	14 (63.6)	21 (72.4)	35 (68.6)

All values are mean (range), unless indicated otherwise.
[a]As calculated in the final population PK model, including the maturation factor.

from the central compartment. This distribution was described by a steady-state intracellular-to-plasma ratio ($R_{IC:P}$) plus intracellular distribution rate constant between plasma and intracellular PBMC compartment (k_{P-IC}) (Figure 1, Equation 7, where A_{IC} represents the amount of drug in the intracellular PBMC compartment, A_C the amount of drug in the central compartment and V_c the volume of distribution of the central compartment).

$$\frac{dA_{IC}}{dt} = k_{P-IC} \cdot \left(R_{IC:P} \cdot \frac{A_c}{V_c} - A_{IC} \right) \quad (7)$$

Final parameter estimates are presented in Table 2. The $R_{IC:P}$ was found to be 2.17 (95% CI 1.98–2.39), indicating an ∼2-fold higher intracellular PBMC miltefosine concentration compared with plasma. The delayed distribution was described with the k_{P-IC} of 1.23 (95% CI 0.94–1.58) day^{-1}. The mean of the individual estimates of $R_{IC:P}$ and k_{P-IC} were comparable between adults and children ($R_{IC:P}$ of 2.3 and 2.2, and k_{P-IC} of 1.2 and 1.3, respectively).

Allometric scaling of V_c and CL by FFM significantly improved the fit compared with scaling by total body weight (ΔOFV −12). Inclusion of the maturation component in FFM calculation improved the model significantly (ΔOFV −7.5). Other evaluated covariates did not improve the model.

Standard goodness-of-fit plots (Figures S1 and S2, available as Supplementary data at *JAC* Online) indicated no obvious deviations, except for a slight overprediction of the highest plasma concentrations after inclusion of intracellular PBMC data in the final model. The VPC of the final population PK model showed good predictive performance of the model compared with the observations (Figure 2).

Using the final population parameter estimates, the plasma elimination half-lives were calculated to be 3.5 days, 7.6 days and a terminal elimination half-life of 51 days. Secondary PK parameters related to exposure were calculated from individual exposure estimates of the 51 patients in the final model (Table 3). Plasma and intracellular PBMC exposure variables were significantly higher for adults compared with children.

Exploration of exposure–response relationships

Of the 49 patients included in the exposure–response analysis, 5 paediatric patients presented with treatment failure. Exploration of the contribution of individual exposure variables to treatment outcome indicated a significant influence of all exposure values (both plasma and intracellular PBMC exposure) on probability of cure, except time>IC_{50} for intracellular PBMC miltefosine concentrations (Table 4). As an example, each 10 mg·day/L increase in $AUC_{PL,\ D0-D28}$ resulted in an increased OR for cure of 1.64 (95% CI 1.18–3.09, λ_B=−23.6). Probability of failure (calculated with Equations 4 and 5) increased from 0.06% to 22.6% for a decrease in $AUC_{PL,\ D0-D28}$ from the median value 623 mg·day/L to 500 mg·day/L. Based on this analysis, the $AUC_{PL,\ D0-D28}$ should exceed 535 mg·day/L to reach >95% probability of cure. The $AUC_{PL,\ D0-D28}$ of all adults in our analysis exceeded this potential PK target, but 12/28 children (43%) did not attain this value. Probability of clinical cure as a function of the $AUC_{PL,\ D0-D28}$ is depicted in Figure 3. The wide CIs reflect the small number of patients that failed treatment.

Baseline lesion size, number of lesions, time of lesion duration prior to treatment, age, gender and isolated strain susceptibility data were not significantly associated with log odds of cure in the multivariate analysis, on top of miltefosine exposure.

Allometric dosing simulation

$AUC_{PL,\ D0-D28}$ values following simulations of linear and allometric dosing regimens are provided in Table 5. Allometric dosing of

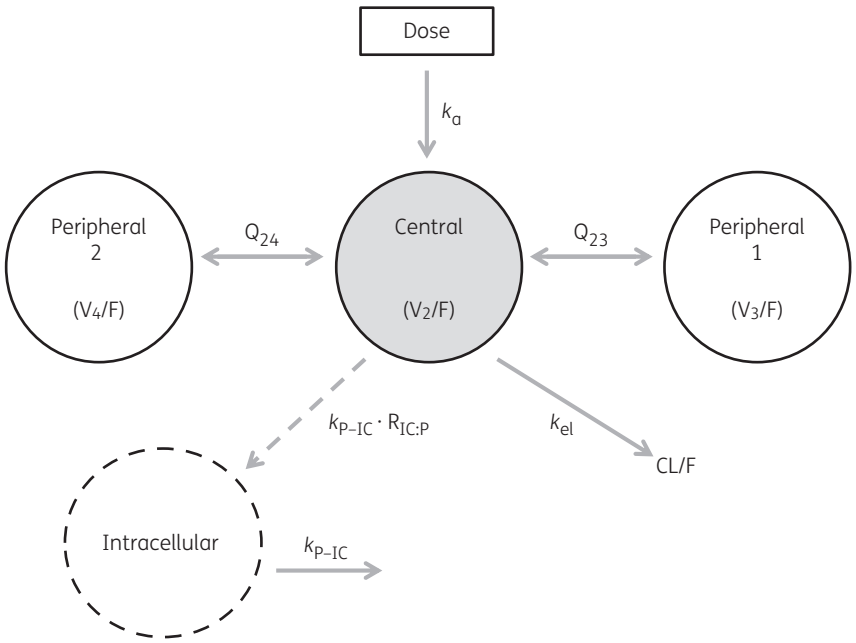

Figure 1. Schematic representation of structural population PK model of miltefosine in cutaneous leishmaniasis patients. V_2 represents the central *V*. V_3 and V_4 represent the two peripheral compartments, and Q_{23} and Q_{24} their respective intercompartmental clearances. Intracellular represents the intracellular effect compartment within PBMCs. F, bioavailability.

Table 2. Parameter estimates of final population PK model

Parameter	Population estimate (%RSE)	95% CI[a]	BSV (%RSE)	95% CI[a]	Shrinkage (%)
k_a, day^{-1}	9.6[b]	–	NE		
Clearance (CL/F)[a], L/day	4.62 (2.8)	4.38–4.88	15.2 (11.4)	11.7–18.5	2.1
Volume of central compartment (V_2/F)[c], L	28.5 (3.3)	26.7–30.3	11.0 (19.4)	6.1–14.7	32.5
Intercompartmental clearance, central volume –peripheral compartment 1 (Q_{23}/F), L/day	0.42 (17.8)	0.29–0.59	NE		
Volume peripheral compartment 1 (V_3/F), L	3.85 (12.9)	2.97–4.93	NE		
Intercompartmental clearance, central volume –peripheral compartment 2 (Q_{24}/F), L/day	0.0274 (6.4)	0.0241–0.0311	NE		
Volume of peripheral compartment 2 (V_4/F), L	2.02 (4.9)	1.85–2.23	NE		
Intracellular distribution rate constant (k_{P-IC}), day^{-1}	1.23(13.5)	0.94–1.58	45.0 (31.6)	1.7–65.3	27.3
Intracellular-to-plasma ratio ($R_{IC:P}$)	2.17 (4.9)	1.98–2.39	28.6 (15.1)	19.8–36.6	11.2
Proportional residual error plasma (%)	16.3 (6.3)	14.4–18.4			9.8
Proportional residual error intracellular (%)	29.3 (6.2)	25.8–32.9			17.7

NE, not estimated.
[a]95% CIs were calculated by the percentile method from bootstrap ($n = 1000$).
[b]Due to absence of sampling in the absorption phase, this was fixed to a previously established value of 9.6.
[c]Estimates are provided for patients with an FFM of 53 kg.

miltefosine resulted in similar exposure levels between children and adults in this patient cohort. Simulating allometric dosing, the fraction of children not attaining the proposed $AUC_{PL,\ D0–D28}$ threshold of 535 mg·day/L was an order of magnitude lower at 1.8%, compared with 18.3% after simulating the linear dose.

Discussion

We report a compartmental population PK model characterizing the pharmacokinetics of miltefosine in plasma and PBMCs and, based on this model, describe the population pharmacokinetics of miltefosine in adults and children with cutaneous leishmaniasis.

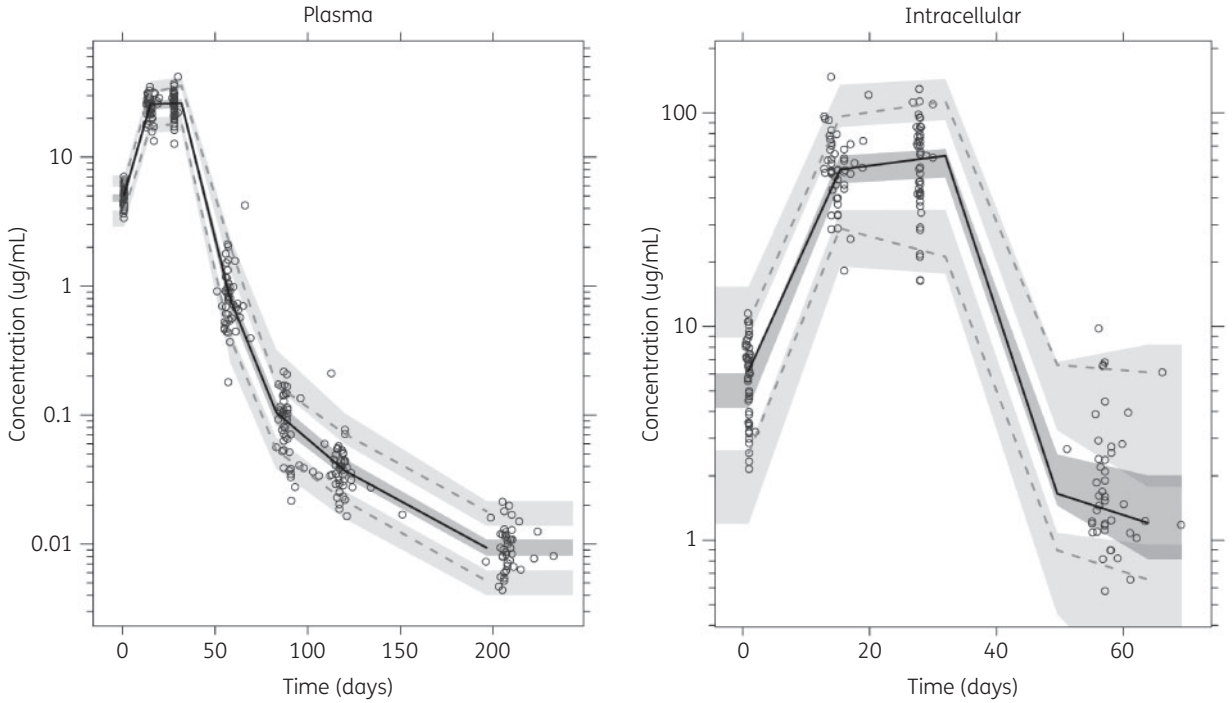

Figure 2. VPC of the final population PK model for plasma miltefosine concentrations (left) and intracellular PBMC miltefosine concentrations (right). Open circles represent individual observations and solid/dashed lines show the median and 5th/95th percentiles of the observed data. Dark/light-grey shadings indicate 95% CIs of predicted median and 5th/95th percentiles.

Table 3. Secondary PK parameters calculated from individual exposure estimates of 51 patients included in the final population PK model

Parameter	Adults (mean±SD)	Children (mean±SD)	*P* value[a]
$C_{max,\ PL}$ (mg/L)	34.1±6.8	22.5±3.8	**4.162e−08**[b]
$C_{max,\ IC}$ (mg/L)	79.9±22.2	47.8±17.3	**1.559e−07**[c]
$AUC_{PL,\ D0–D28}$ (mg·day/L)	789±102	545±64	**2.114e−11**[b]
$AUC_{IC,\ D0–D28}$ (mg·day/L)	1707±374	1169±379	**4.815e−06**[c]
$AUC_{PL,\ 0–\infty}$ (mg·day/L)	1056±164	688±94	**1.205e−10**[b]
$AUC_{IC,\ 0–\infty}$ (mg·day/L)	2405±635	1533±517	**4.099e−07**[c]
$AUC{>}IC_{50,\ PL,\ 0–\infty}$ (mg·day/L)	934±154	577±89	**5.725e−11**[b]
$AUC{>}IC_{50,\ IC,\ 0–\infty}$ (mg·day/L)	2259±620	1398±506	**3.129e−07**[c]
$Time{>}IC_{50,\ PL,\ 0–\infty}$ (days)	51±5	44±3	**1.011e−07**[c]
$Time{>}IC_{50,\ IC,\ 0–\infty}$ (days)	61±7	54±6	**2.597e−04**[d]

C_{max}, miltefosine concentration on the last treatment day.
[a]Bold text indicates $P < 0.001$.
[b]Welch two-sample *t*-test.
[c]Wilcoxon rank sum test.
[d]Two-sample *t*-test.

The observed plasma and intracellular PBMC miltefosine concentrations were well described and predicted by the population PK model. PK parameter estimates of the final model were in line with values previously reported.[5–7] The V_c was smaller than previously documented (28.5 L versus 38.5–40.1 L), due to the inclusion of a second peripheral compartment.[5–7] The two peripheral compartments were required to accurately describe the observed multiphasic elimination phase. Triphasic elimination has never been observed previously for miltefosine[5] and was possibly influenced by denser sampling in the first 3 months after treatment in the current study.

Implementation of $k_{P–IC}$ was required to characterize the delay in intracellular PBMC miltefosine distribution. In Caco-2 cells, only 6.8% of miltefosine was transported across cells after a 3 h incubation, whereas 57% accumulated in the membranes, from which intracellular release was slow (5% in 24 h).[3] Inward translocation of miltefosine within the cellular membrane was found *in vitro* to be partially dependent on active saturable transport.[3,4] These sequential processes could hypothetically explain the delayed intracellular PBMC miltefosine distribution, potentially leading to variability in the extent of intracellular PBMC distribution amongst patients. Redistribution of miltefosine during washing of the cells upon harvesting is not expected to have affected the intracellular concentrations, because all washing steps were short, under cold conditions, whereas miltefosine's lipophilicity probably favours the cell membrane.

Compared with the previously reported model-based $AUC_{PL,\ D0–D28}$ estimate of ∼500 mg·day/L for Indian paediatric visceral leishmaniasis patients,[6] the $AUC_{PL,\ D0–D28}$ estimate for paediatric patients in this study was 9% higher (545 mg·day/L). As this is a relatively small difference, large variations between these two patient populations in PK characteristics such as metabolism and distribution of miltefosine are not expected, although these could

Table 4. Logistic regression analysis of exposure variables affecting the probability of clinical cure after miltefosine monotherapy in cutaneous leishmaniasis patients

	OR	95% CI	Likelihood ratio significance
$C_{max,\ PL}$ (per mg/L)	1.46	1.12–2.18	$P < 0.01$
$C_{max,\ IC}$ (per mg/L)	1.06	1.00–1.14	$P < 0.05$
$AUC_{PL,\ D0–D28}$ (per 10 mg·day/L)	1.64	1.18–3.09	$P < 0.001$
$AUC_{IC,\ D0–D28}$ (per 10 mg·day/L)	1.04	1.01–1.09	$P < 0.05$
$AUC_{PL,\ 0–\infty}$ (per 10 mg·day/L)	1.32	1.09–1.93	$P < 0.001$
$AUC_{IC,\ 0–\infty}$ (per 10 mg·day/L)	1.03	1.01–1.08	$P < 0.01$
$AUC>IC_{50,\ PL,\ 0–\infty}$ (per 10 mg·day/L)	1.41	1.11–2.21	$P < 0.001$
$AUC>IC_{50,\ IC,\ 0–\infty}$ (per 10 mg·day/L)	1.03	1.01–1.08	$P < 0.01$
$Time>IC_{50,\ PL,\ 0–\infty}$ (per day)	1.34	1.03–1.93	$P < 0.05$
$Time>IC_{50,\ IC,\ 0–\infty}$ (per day)	1.12	0.96–1.36	NS

NS, not significant.

Table 5. Exposure to miltefosine as $AUC_{PL,\ D0–D28}$, simulated for Colombian cutaneous leishmaniasis patients with the final population PK model after linear and allometric dosing, for both adults and children

Age category	$AUC_{PL,\ D0–D28}$, mg·day/L, mean (95% CI)	Percentage of population below the 95% probability of cure exposure threshold[a]
Linear dosing		
Children (≤12 years)	629 (437–858)	18.3
Adults (≥18 years)	751 (529–1013)	2.8
Allometric dosing		
Children (≤12 years)	708 (545–903)	1.8
Adults (≥18 years)	693 (521–883)	3.5

[a]535 mg·day/L $AUC_{PL,\ D0–D28}$.

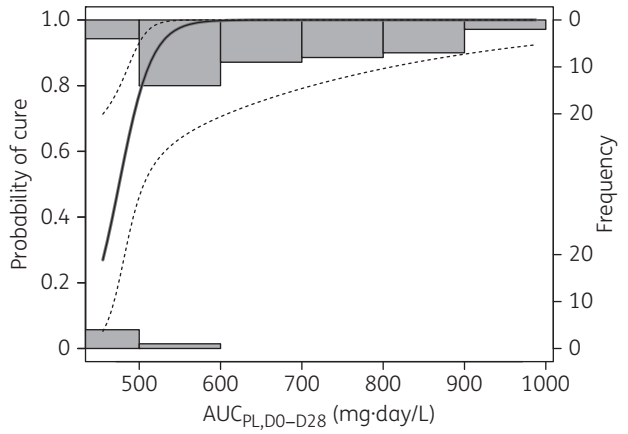

Figure 3. Probability of clinical cure by miltefosine monotherapy as a function of the plasma AUC up to the end of treatment ($AUC_{PL,\ D0–D28}$). The thick line represents the predicted probability of cure for the patients in this study with the logistic model, and the dotted lines indicate the 95% CI. The histograms represent the observations and indicate the number of patients (frequency) in the corresponding $AUC_{PL,\ D0–D28}$ intervals that are either cured (top of graph) or fail (bottom of graph) after miltefosine monotherapy.

have been anticipated due to differences in clinical presentation (e.g. altered liver physiology in visceral but not cutaneous leishmaniasis).

Although the clinical PK trial from which the current data originated was not powered to evaluate efficacy, our results might provide a potential miltefosine exposure target in treatment of cutaneous leishmaniasis. In contrast to the previous multivariate analysis using NCA PK estimates,[1] population PK model-based estimates of plasma and intracellular PBMC miltefosine exposure were significantly associated with probability of cure. Differences in results between these methodologies could be caused by this trial's restricted sampling scheme designed to comply with ethical requirements of sampling in children. The NCA PK estimates from the previous analysis therefore underestimate the $AUC_{PL,\ D0–D28}$ (e.g. for children, 456±100 mg·day/L compared with the 545±64 mg·day/L model-based estimate). Differences in results between these methodologies could not be explained by exclusion of the eight potentially non-adherent patients in the population PK model, as the NCA exposure–response relation remained not significant when excluding these patients (data not shown).

In this study, both plasma and intracellular PBMC miltefosine exposure were significantly related to probability of cure, which can be expected as plasma and intracellular PBMC concentrations are highly correlated. In future clinical studies, intracellular PBMC exposure could potentially be predicted from plasma PK using the here-developed population PK model. It might be valuable to relate intracellular PK to individual IC_{50} (or IC_{90}) values from clinical parasite strains to calculate individual time>IC_{50} and AUC>IC_{50} exposure variables. Exploration of these intracellular PBMC PK/pharmacodynamic (PD) relationships could aid in understanding the contribution of *Leishmania* drug susceptibility to individual therapeutic outcome.

Ex vivo IC_{50} values of previously isolated clinical strains of *L.V. panamensis* varied widely with a median (range) of 1.9 (0.53–13) mg/L.[16] The median 1.9 mg/L IC_{50} value used in the current analysis provides a first approximation (to our knowledge) that can be evaluated and adjusted based on future drug susceptibility studies. In a sensitivity analysis increasing IC_{50} values up to 13 mg/L, there were no profound differences in the PK/PD relationship, except that time>$IC_{50,IC,\ 0–\infty}$ was a significant predictor of cure above a certain level (data not shown). We aimed to capture the variability in susceptibility by including individual miltefosine susceptibility scores (% parasite load reduction after *ex vivo* exposure to 16 μM)[16] as a covariate effect on probability of cure in addition to drug exposure. No significant effect was identified, possibly due to the small sample size and unavailable susceptibility data for *Leishmania* strains that were not isolated from two out of five patients who failed treatment. Drug susceptibility values are influenced by a multitude of factors, including type of host cell.[17] It

should be noted that the current analysis used values derived from studies using human macrophages differentiated from U937 cells.

Lastly, model-based simulations showed that an allometric dose regimen would result in a higher probability of reaching the proposed $AUC_{PL,\ D0–D28}$ threshold of 535 mg·day/L for children. The safety of this allometric regimen is currently being evaluated in East Africa (NCT02431143) and Bangladesh (NCT02193022). Differences in simulated (82%, Table 4) versus observed target attainment (57%) in children after conventional dosing could be explained by the lower administered daily dose of 2.3 mg/kg (Table 1, range 2.0–2.5 mg/kg) compared with the simulated 2.5 mg/kg.[1] Additionally, the 90%–100% range of adherence to treatment for patients in this study[1] could also have contributed to lower observed target attainment compared with simulations with 100% adherence.

In conclusion, we developed a population PK model, which in addition to plasma miltefosine pharmacokinetics also describes the intracellular kinetics in PBMCs, characterizing miltefosine exposure in a compartment that is a closer approximation of miltefosine's *in vivo* target site of action. In the future, the model can be used in predicting individual intracellular PBMC concentration data, which can subsequently be related to individual *Leishmania* drug susceptibility to identify its impact on therapeutic outcome. In the here-presented exploratory exposure–response analysis, both plasma and intracellular PBMC miltefosine exposure parameters were significantly associated with probability of cure. A 535 mg·day/L $AUC_{PL,\ D0–D28}$ threshold could be proposed from our analysis as a putative PK target; however, its validity should be evaluated in a larger cohort of patients. The developed model can be exploited for analyses of PK/PD relationships in these future trials.

Acknowledgements

We gratefully acknowledge the patients and parents of the children who participated in this study and the support of community leaders in Tumaco. We would like to recognize the technical and logistic support of the clinical and laboratory team of CIDEIM in Cali and Tumaco: Eduardo Ortiz, Adriana Navas, Angelica Mera, Jimena Jojoa, Wilson Cortes, Mary Luz Hurtado and Mabel Castillo. We thank Dr Robert Vinson and Paladin Labs Inc. for the generous donation of Impavido® for this study.

Funding

This work was funded by the Colombian National Administrative Department of Science, Technology and Innovation (COLCIENCIAS) (grant number 2229-519-28930 and institutional strengthening contract 718-2013), and partially supported by US National Institutes of Health (NIH) (Grants R01AI104823 and R01AI093775), and US NIH International Fogarty Center Global Infectious Disease Research Training Program (Award Number D43 TW006589). M. d. M. C. was a recipient of COLCIENCIAS Young Investigator Award [0040–2012]. T. P. C. D. is personally financially supported by the Netherlands Organisation for Scientific Research (NWO-ZonMw), Veni programme (project no. 91617140).

Transparency declarations

None to declare.

Supplementary data

Figures S1 and S2 appear as Supplementary data at *JAC* Online.

References

1 Castro MM, Gomez MA, Kip AE *et al*. Pharmacokinetics of miltefosine in children and adults with cutaneous leishmaniasis. *Antimicrob Agents Chemother* 2016; **61**: e02198-16.

2 Dorlo TPC, Balasegaram M, Beijnen JH *et al*. Miltefosine: a review of its pharmacology and therapeutic efficacy in the treatment of leishmaniasis. *J Antimicrob Chemother* 2012; **67**: 2576–97.

3 Ménez C, Buyse M, Dugave C *et al*. Intestinal absorption of miltefosine: contribution of passive paracellular transport. *Pharm Res* 2007; **24**: 546–54.

4 Ménez C, Buyse M, Farinotti R *et al*. Inward translocation of the phospholipid analogue miltefosine across Caco-2 cell membranes exhibits characteristics of a carrier-mediated process. *Lipids* 2007; **42**: 229–40.

5 Dorlo TPC, van Thiel PPAM, Huitema ADR *et al*. Pharmacokinetics of miltefosine in Old World cutaneous leishmaniasis patients. *Antimicrob Agents Chemother* 2008; **52**: 2855–60.

6 Dorlo TPC, Huitema ADR, Beijnen JH *et al*. Optimal dosing of miltefosine in children and adults with visceral leishmaniasis. *Antimicrob Agents Chemother* 2012; **56**: 3864–72.

7 Dorlo TPC, Rijal S, Ostyn B *et al*. Failure of miltefosine in visceral leishmaniasis is associated with low drug exposure. *J Infect Dis* 2014; **210**: 146–53.

8 Charles B. Population pharmacokinetics: an overview. *Aust Prescr* 2014; **37**: 210–3.

9 Kip AE, Rosing H, Hillebrand MJX *et al*. Quantification of miltefosine in peripheral blood mononuclear cells by high-performance liquid chromatography-tandem mass spectrometry. *J Chromatogr B Analyt Technol Biomed Life Sci* 2015; **998–999**: 57–62.

10 Dorlo TPC, Hillebrand MJX, Rosing H *et al*. Development and validation of a quantitative assay for the measurement of miltefosine in human plasma by liquid chromatography-tandem mass spectrometry. *J Chromatogr B Analyt Technol Biomed Life Sci* 2008; **865**: 55–62.

11 Simiele M, D'Avolio A, Baietto L *et al*. Evaluation of the mean corpuscular volume of peripheral blood mononuclear cells of HIV patients by a coulter counter to determine intracellular drug concentrations. *Antimicrob Agents Chemother* 2011; **55**: 2976–8.

12 Kjellsson MC, Via LE, Goh A *et al*. Pharmacokinetic evaluation of the penetration of antituberculosis agents in rabbit pulmonary lesions. *Antimicrob Agents Chemother* 2012; **56**: 446–57.

13 Clewe O, Goutelle S, Conte JE Jr *et al*. A pharmacometric pulmonary model predicting the extent and rate of distribution from plasma to epithelial lining fluid and alveolar cells—using rifampicin as an example. *Eur J Clin Pharmacol* 2015; **71**: 313–9.

14 Janmahasatian S, Duffull SB, Ash S *et al*. Quantification of lean bodyweight. *Clin Pharmacokinet* 2005; **44**: 1051–65.

15 Al-Sallami HS, Goulding A, Grant A *et al*. Prediction of fat-free mass in children. *Clin Pharmacokinet* 2015; **54**: 1169–78.

16 Fernandez O, Diaz-Toro Y, Valderrama L *et al*. Novel approach to in vitro drug susceptibility assessment of clinical strains of *Leishmania* spp. *J Clin Microbiol* 2012; **50**: 2207–11.

17 Seifert K, Escobar P, Croft SL. *In vitro* activity of anti-leishmanial drugs against *Leishmania donovani* is host cell dependent. *J Antimicrob Chemother* 2010; **65**: 508–11.